LIMD2 promotes tumor proliferation, invasion, and epithelial-mesenchymal transition in clear cell renal cell carcinoma

Qi-Yu ZHONG[1,2,#], Ying-Wei XIE[3,#], Zhi-Liang CHEN[1,2], Yu-Qing CHEN[4], Yue-Xin LIU[3], Wen-Lian XIE[1,2,5,*], Wei YAN[3,*]

[1]*Department of Urology, Sun Yat-Sen Memorial Hospital, Sun Yat-Sen University, Guangzhou, China;* [2]*Guangdong Provincial Key Laboratory of Malignant Tumor Epigenetics and Gene Regulation, Sun Yat-Sen Memorial Hospital, Sun Yat-Sen University, Guangzhou, China;* [3]*Department of Urology, Beijing Tongren Hospital, Capital Medical University, Beijing, China;* [4]*Department of Pathology, Sun Yat-Sen Memorial Hospital, Sun Yat-Sen University, Guangzhou, China;* [5]*Guangdong Provincial Clinical Research Center for Urological Diseases, Sun Yat-Sen Memorial Hospital, Sun Yat-Sen University, Guangzhou, China*

*Correspondence: yanweiuro@126.com; xiewl@mail.sysu.edu.cn
#Contributed equally to this work.

LIMD2 was found upregulated in various tumors and metastatic samples and associated with a poor prognosis. But the role of LIMD2 in clear cell renal cell carcinoma (ccRCC) remains elusive. The expression of LIMD2 in ccRCC was analyzed using cohort data downloaded from TCGA and ICGC databases. *In vitro* and *in vivo* experiments were then conducted to study the biological role of LIMD2 in ccRCC and explore the possible mechanism. The results indicated that LIMD2 was overexpressed and correlated with a poor outcome in ccRCC. LIMD2 promoted the malignancy of ccRCC both *in vitro* and *in vivo*. LIMD2 induced epithelial-mesenchymal transition (EMT) via activating the ILK/Akt pathway in ccRCC. In conclusion, LIMD2 is overexpressed and promotes proliferation, invasion, and EMT in ccRCC, which may serve as a potential novel therapeutic target for ccRCC.

Key words: LIM domain protein 2, epithelial-mesenchymal transition, clear cell renal cell carcinoma, proliferation, invasion

Renal cell carcinoma (RCC) is one of the most common urological malignant neoplasms, ranking 6th in men and 8th in women [1]. And clear cell renal cell carcinoma (ccRCC), the most common subtype, accounts for over three-quarters of RCC cases [2]. In the early stage of ccRCC, symptoms are not obvious enough and surgery remains the mainstay of curative treatment [3, 4]. However, up to a third of cases have distant metastases already when diagnosis is made, leading to a poor prognosis [3]. Moreover, tumor recurrence or metastasis could also be found in nearly 30% of those who had already undergone surgery [5]. Therefore, seeking novel molecular targets and exploring the mechanism of ccRCC metastasis is in urgent need.

LIM domain proteins are a large family of proteins with diverse cellular roles and emerging as vital key molecules in various cancers [6]. LIMD2, a member of the LIM domain-proteins family, is found to be overexpressed in a variety of malignant human tumors and metastasis samples [7]. LIMD2 can promote tumor progression, metastatic process, and is linked to a poor prognosis [8–12]. Moreover, LIMD2 potentiates its biologic function via directly interacting with integrin-linked kinase (ILKs), then promotes cell motility

and tumor progression [8]. However, research on the biological function of LIMD2 in ccRCC remains limited. In this research, we found the augmenting expression levels of LIMD2 in ccRCC, which promotes the tumor proliferation, invasion as well as metastasis of ccRCC.

Patients and methods

Patients and tissue samples. This study was approved by the Research Ethics Committee of Sun Yat-Sen Memorial Hospital (SYSMH), Sun Yat-Sen University and was conducted in accordance with the tenets of the Declaration of Helsinki. ccRCC tissues and adjacent no-cancerous tissues were obtained from 83 patients who underwent surgery at SYSMH. Written informed consent has been obtained from each patient. Tumor tissues and adjacent normal tissues were pathologically confirmed by two pathologists. All fresh tissues were snap-frozen immediately in liquid nitrogen after collection and stored at –80 °C.

Reagents and antibodies. The antibodies used for western blotting are listed as follows: mouse anti-GAPDH (51332, 1:1000, CST), rabbit anti-E-cadherin (3195, 1:1000, CST),

rabbit anti-N-cadherin (13116, 1:1000, CST), rabbit anti-Slug (9585, 1:1000, CST), rabbit anti-Snail (3879, 1:1000, CST), rabbit anti-AKT (pan, 11E7, 1:1000, CST), rabbit anti-p-AKT (Ser473, 4060, 1:1000, CST), rabbit anti-LIMD2 (ab205375, 1:1000, Abcam), and mouse anti-ILK (sc20019, 1:1000, Santa Cruz Biotechnology). Recombinant human LIMD2 protein (LS-G20929) was purchased from LSBio (Seattle, USA). ILK inhibitor OSU-T315 was obtained from Selleck Chemicals (Shanghai, China).

Cell lines and cell culture. The human ccRCC cell lines Caki-1, 769-p, and normal kidney cell line HK-2 were obtained from the American Type Culture Collection (ATCC, Manassas, USA). Caki-1 and 769-p cells were cultured in DMEM (Gibco, USA). HK-2 cells were cultured in DMEM/F12 (Gibco, USA). All culture media was supplemented with 10% fetal bovine serum (FBS, Gibco, USA) and 1% penicillin/streptomycin (Hyclone, USA). Cells were cultured in a humidified 5% CO_2 incubator at 37 °C.

Cell transfection, lentivirus production, and infection. 769-p and Caki-1 cells were transiently transfected with 100 nM negative control (NC) siRNA or LIMD2-targeting siRNA (Genepharma. Suzhou, China), using Lipofectamine™ RNAiMAX Transfection Reagent (Invitrogen, USA) according to the manufacturer's protocol. The target sequences in this study were as follows: si#1: 5'-GCUUCUGCUGCAAGCA-CUGTT-3', 5'-CAGUGCUUGCAGCAGAAGCTT-3'; si#2: 5'-GCAGCUGUUUAAGAGCAAATT-3', 5'-UUUGCUCU-UAAACAGCUGCTT-3'.

Using BLOCK-iT™ RNAi Designer (Invitrogen, USA) to convert siRNA (si#1) sequences to shRNA oligo sequences. LIMD2 shRNA was cloned into the pLKO.1-puro vector (Igebio, Guangzhou, China) and then co-transfected with lentiviral packaging plasmids pMD2.G and psPAX2 into 293T cells for lentivirus production. Caki-1 cells were infected with the lentivirus, followed by a 3 μg/ml puromycin selection to generate a stable knockdown cell line. The shRNA sequences were as follows: Top: 5'-CACCGCTTCTGCTGCAAGCACT-GTTCGAAAACAGTGCTTGCAGCAGAAGC-3'; Bottom: 5'-AAAAGCTTCTGCTGCAAGCACTGTTTTCGAA-CAGTGCTTGCAGCAGAAGC-3'.

RNA extraction and RT-qPCR assays. Total RNA was extracted from tumor tissues or cultured cells using RNAiso Plus (Takara, Japan) and then transcribed to cDNA using an Evo M-MLV RT Kit for qPCR (Accurate Biotech, Hunan, China). RT-qPCR was performed on LightCycler 96 real-time PCR system (Roche, Switzerland) using a SYBR Green Premix Pro Taq HS qPCR Kit (Accurate Biotech, Hunan, China). The thermocycling conditions were: 95 °C for 30 s, followed by 40 times of 95 °C for 5 s and 60 °C for 30 s. The transcription expression of GAPDH was used as an internal control. The comparative $2^{-\Delta\Delta Cq}$ method was utilized for relative quantification. The primer sequences are listed as follows: GAPDH: F: 5'-CTGGGCTACACTGAGCACC-3'; R: 5'-AAGTGGTC-GTTGAGGGCAATG-3'; LIMD2: F: 5'-TGCCAGAAGACC-GTGTACC-3; R: 5'-TTTGCAGTAGAACTCCCCGTG-3'.

MTS and colony formation assays. Cell proliferation was evaluated by the MTS assay. Transfected cells ($1.0×10^3$ /well) were seeded in 96-well plates and cultured at 37 °C. Then 20% MTS solution (CellTiter96® AQueous One Solution Cell Proliferation Assay, Promega, USA) was added to each well, followed by the incubation for 2 h in the dark. The optical density of the cells was then measured at 490 nm. The measurements were conducted every 24 h for 6 days.

For the colony formation assays, transfected cells, at the density of $1.0×10^3$ cells/well, were inoculated onto 6-well plates and cultured for 2 weeks. The medium was replaced with fresh medium every 3–4 days. After washing with PBS, the visible colonies were fixed by 4% paraformaldehyde, stained by 0.1% crystal violet, and then manually counted.

Wound-healing assays. $1.0×10^5$ cells/well of transfected cells were plated in 12-well plates. Once cells reached 90% confluency, a 200 μl sterile pipette tip was used to scratch the cell surface and create the wound. After washing twice with PBS, the cells were cultured in an FBS-free medium. The wound formation was observed under an inverted microscope and photographed at 0 and 24 h.

Transwell assays. For Transwell assays, $1.0×10^5$ cells suspended in an FBS-free medium were seeded in the upper chamber of a 24-well Transwell chamber (3422, Corning, USA). All lower chambers were filled with a complete culture medium containing 10% FBS. For migration assays, the upper chambers were non-coated. For invasion assays, the upper chambers were pre-coated with Matrigel (1:8 diluted, BD Biosciences, USA). The migrating cells passing through the polycarbonate membrane after 5 h, and the invasive cells after 48 h were then fixed with 4% paraformaldehyde, stained with 0.1% crystal violet solution, and counted at a 100× magnification in 3 randomly selected areas.

Xenografts experiments. All animal experiments were approved by the Institutional Animal Care and Use Committee of Sun Yat-Sen Memorial Hospital, Sun Yat-Sen University, and conducted in accordance with the guidelines of the National Institutes of Health guide for the care and use of laboratory animals. The 5-week-old male BALB/c nude mice were purchased from the Experimental Animal Center of Sun Yat-Sen University and randomly divided into sh-NC and sh-LIMD2 groups (n=5/group). Approximately $5.0×10^6$ Caki-1 cells stably transfected with sh-NC or sh-LIMD2 were suspended in 100 μl PBS and then subcutaneously injected into the upper back of mice. The tumor volume was calculated weekly according to the following formula: V = $(W^2×L)/2$. At the end of the experiment, mice were euthanized, and tumors were harvested, weighed, and processed for immunohistochemistry (IHC).

IHC analysis. Tumors harvested from xenografts experiments were fixed with paraformaldehyde and embedded in paraffin. These sample sections were blocked in normal goat serum for 30 min, incubated with rabbit anti-Ki67 antibody (ZA-0502, ZSBio, China) overnight at 4 °C, and stained by DAB Detection Kit (PV-6000D, ZSBio, China) and hematox-

ylin. The stained cells were counted and the percentage of positive cells was calculated for statistical analysis.

Western blotting analysis. Total proteins were isolated from cells with RIPA lysis buffer, separated by 10% SDS-PAGE gels, and transferred onto the PVDF membranes. After blocking with 5% BSA solution at room temperature for 1 h, the membranes were then incubated with specific primary antibodies overnight at 4°C. Next, the blots were incubated with secondary antibodies for 1 h at room temperature. The protein bands were visualized using Immobilon Western Chemiluminescent HRP Substrate (Millipore, USA) and photographed.

Bioinformatics analysis. TCGA (https://portal.gdc.cancer.gov/) and ICGC (https://dcc.icgc.org/) databases are used in this study. Since the cohort data was obtained from open public databases, ethical approval is not required. The R package "*cgdsr*" was used to download the cohort data of ccRCC patients from TCGA and ICGC databases, including their gene expression data and clinicopathological parameters. R software was applied for data analysis. The statistical significance of these clinical features was tested using the Wilcoxon rank sum test or Kruskal-Wallis rank sum test. The R package "*survminer*" was utilized to screen out 500 patients with at least 90 days of follow-up time in TCGA cohort. The expression dataset was sourced from TCGA and divided into a high-expression group and a low-expression group according to the median expression level of LIMD2 (n=258/group). Gene set enrichment analysis was performed in the Hallmarks gene set database using GSEA 4.1.0 software (Broad Institute, California, USA).

Statistical analysis. All experiments were performed in triplicate, and SPSS 20.0.0 software (IBM, Chicago, USA) was applied for statistical analysis. Quantitative variables were expressed as mean ± SD. The significance between two groups was determined by Student's t-test and the significance of clinical characteristics was determined by the t-test and χ^2-test. Kaplan-Meier method and log-rank test were used for survival analysis. A p-value <0.05 was considered statistically significant.

Results

LIMD2 is overexpressed in ccRCC. To identify the biological role of LIMD2 in ccRCC, we firstly analyzed the gene expression data retrieved from TCGA and ICGC databases, including 516 cancer tissue samples versus 72 non-cancer tissue samples in TCGA database and 91 cancer tissue samples versus 45 adjacent no-cancerous tissue samples in ICGC database. We noted that LIMD2 was significantly overexpressed in ccRCC tissues (Figures 1A, 2B). Then, we detected the LIMD2 mRNA expression of 83 paired ccRCC tissues and adjacent normal tissues and ccRCC cell lines. Similarly, LIMD2 was overexpressed in ccRCC tissues (Figure 1C) as well as ccRCC cell lines 769-p and Caki-1 (Figure 1D).
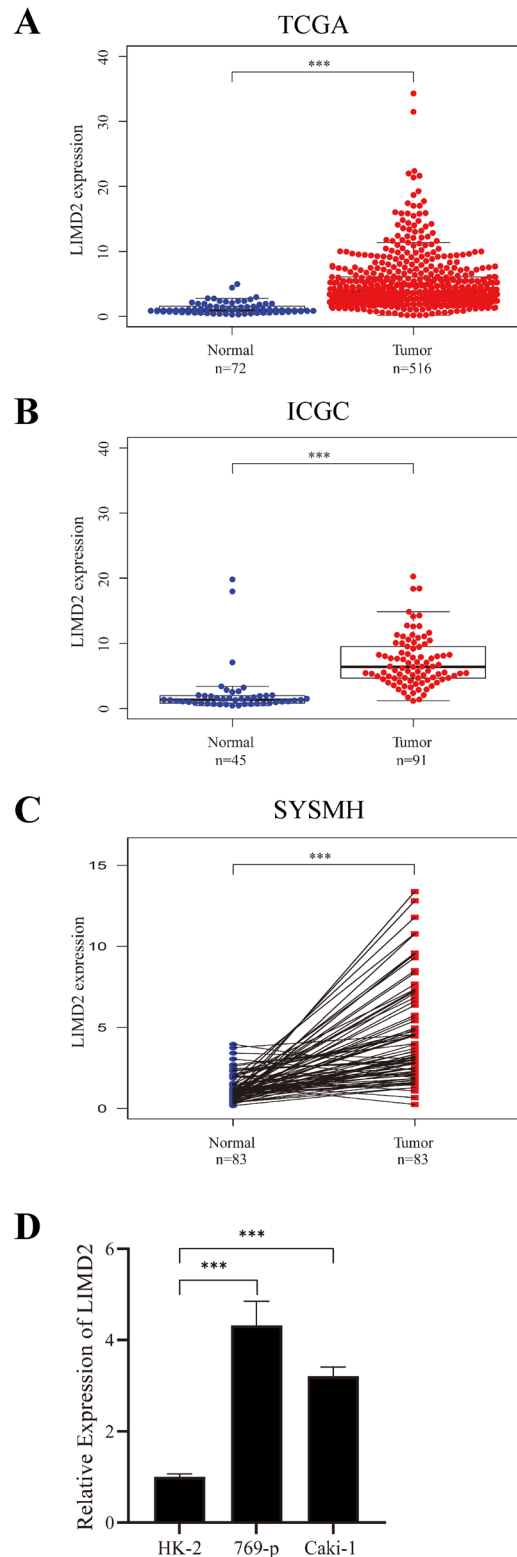

Figure 1. LIMD2 was overexpressed in ccRCC. A) LIMD2 was overexpressed in ccRCC in TCGA database; B) LIMD2 was overexpressed in ccRCC in ICGC database. C) LIMD2 was overexpressed in ccRCC in SYS-MH database. D) LIMD2 was overexpressed in ccRCC cell lines. *p<0.05

Increased LIMD2 expression is correlated with a poor prognosis of ccRCC. Furthermore, analysis of clinicopathological parameters revealed that increased LIMD2 expression was significantly correlated with a higher pathogenic grade and tumor disease stage (Figures 2A–2E, Table 1) both in the SYSMH cohort and TCGA database. Additionally, survival analysis using the Kaplan-Meier method showed that ccRCC patients with high LIMD2 expression had shorter OS in TCGA cohort (Figure 2F). In conclusion, these findings indicate that LIMD2 serves as a critical oncogene and is linked to a poor clinical outcome of ccRCC.

LIMD2 promotes proliferation, migration, and invasion of ccRCC cells *in vitro*. Based on the data above, we further evaluated whether LIMD2 drove tumorigenesis and progression of ccRCC. To reduce the LIMD2 expression in ccRCC cells, we then synthesized two LIMD2-targeting small interference RNAs, si#1 and si#2, which sufficiently downregulated the mRNA and protein expression level of LIMD2 in Caki-1 and 769-p cells respectively (Figure 3A). MTS assays revealed that LIMD2 silencing significantly weakened the proliferation ability of Caki-1 and 769-p cells compared with NC (Figure 3B). Colony formation assays showed that downregulating LIMD2 remarkably reduced cell colonies (Figure 3C). Moreover, LIMD2 knockdown significantly suppressed ccRCC cell migration and invasion ability (Figure 3D, 3E). These results suggest that LIMD2 promotes proliferation, migration, and invasion of ccRCC *in vitro*.

LIMD2 enhances ccRCC tumor growth *in vivo*. To further investigate the oncogenic role of LIMD2 on ccRCC *in vivo*, Caki-1 cells stably transfected with sh-NC or sh-LIMD2 were utilized for establishing xenograft models (n=5/group) (Figure 4A). The results showed that LIMD2 knockdown obviously reduced tumor growth *in vivo* (Figure 4B).

Table 1. Associations between the expression level of LIMD2 and clinicopathological parameters of ccRCC patients.

Characteristics	High Expression (n=54)	Low Expression (n=29)	p-value
Gender			
Male	44	21	0.339
Female	10	8	
Age (years)			
<60	34	22	0.232
≥60	20	7	
Neoplasm stage			
Stage I–II	31	25	0.008*
Stage III–IV	23	4	
T stage			
T1	33	26	0.006*
T2–4	21	3	

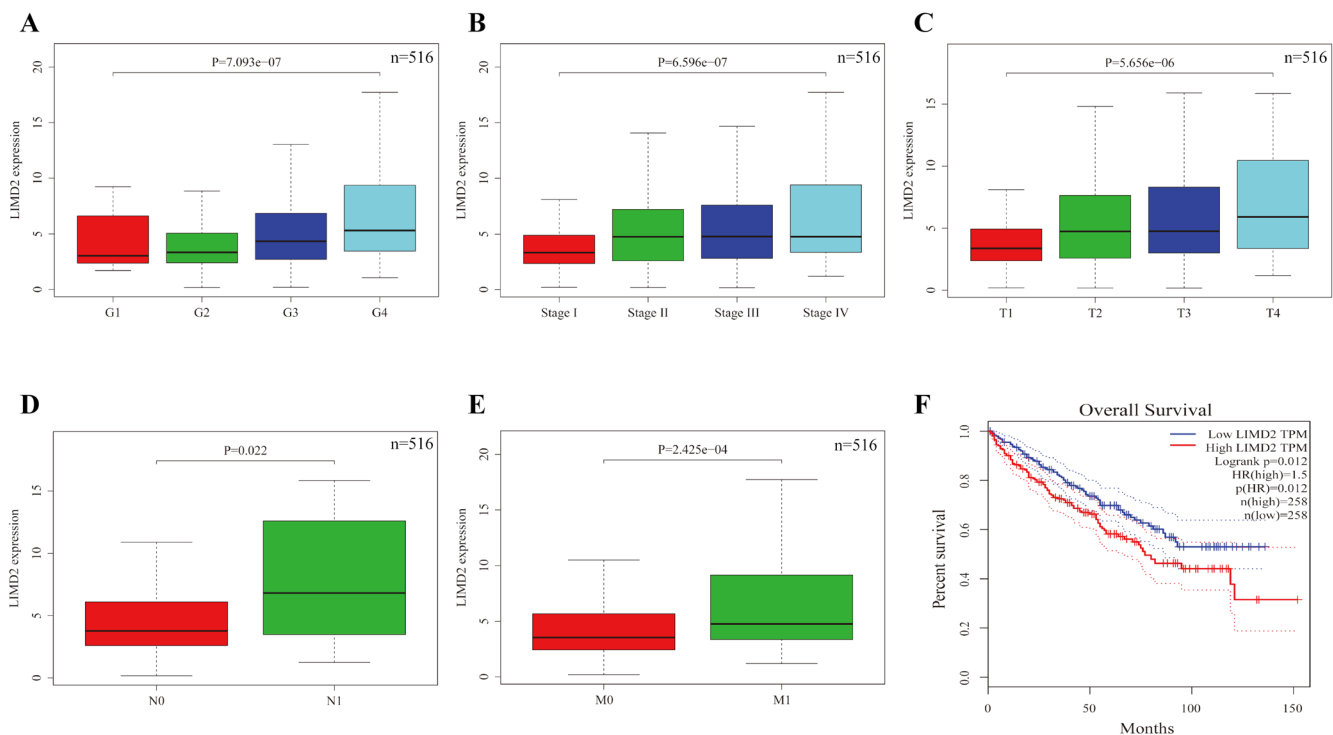Note: *p<0.05 was considered statistically significant

Figure 2. Increased LIMD2 expression was linked to a poor outcome of ccRCC. A) High LIMD2 expression was correlated to a high historical grade in TCGA. B) High LIMD2 expression was linked to a high neoplasm disease stage in TCGA. C–E) High LIMD2 expression was related to a high T (C), M (D), N (E) stage in TCGA. F) ccRCC patients with high LIMD2 expression had shorter OS in TCGA.
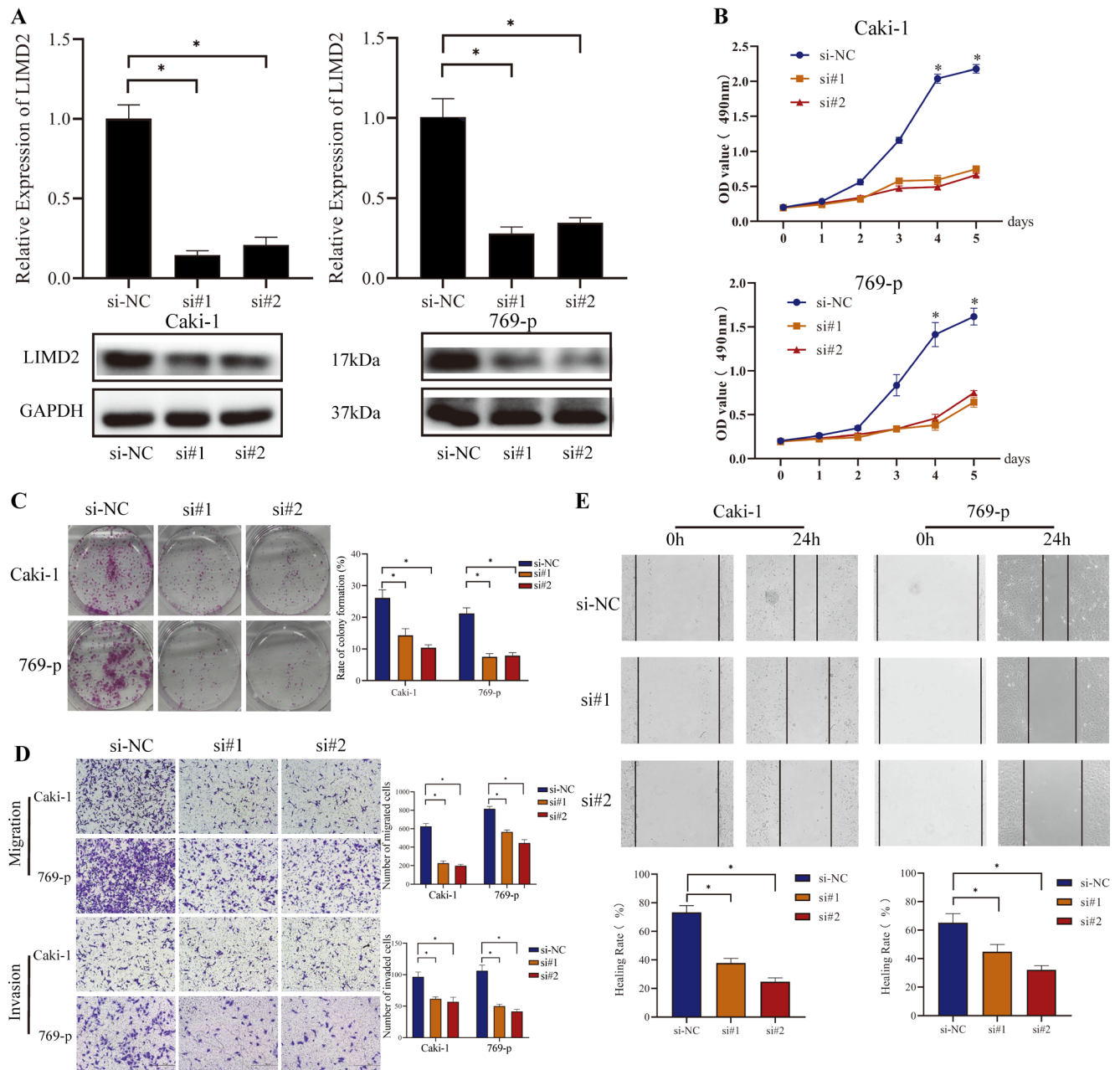
Figure 3. LIMD2 promotes the malignancy of ccRCC cells *in vitro*. A) The efficiencies of LIMD2 knockdown in Caki-1 and 769-p cells. **B)** The cell viability of Caki-1 and 769-p cells after LIMD2 knockdown. **C)** Effects of LIMD2 silencing on colony formation ability in Caki-1 and 769-p cells. **D, E)** The migration and invasion capacity assessed by Transwell assays (D) and wound-healing assays (E) of Caki-1 and 769-p cells with si-LIMD2 transfection. *p<0.05

Tumor volume and weight were significantly decreased in the sh-LIMD2 group compared with the sh-NC group (Figures 4C, 4D). Besides, IHC assays showed that LIMD2 knockdown obviously diminished the numbers of Ki67 (+) cells (Figures 4E, 4F). Taken together, these findings indicate that LIMD2 may play a tumor promotive role in ccRCC both *in vitro* and *in vivo*.

LIMD2 promotes EMT in ccRCC. In order to explore the possible mechanism of LIMD2 in ccRCC, we conducted a gene set enrichment analysis of LIMD2 in the Hallmarks gene set database. As shown in Figure 5A, two of the top ten pathways that positively related to high-LIMD2 expression were "HALLMARK_EPITHELIAL_MESENCHYMAL_ TRANSITION" and "HALLMARK_PI3K_AKT_MTOR_
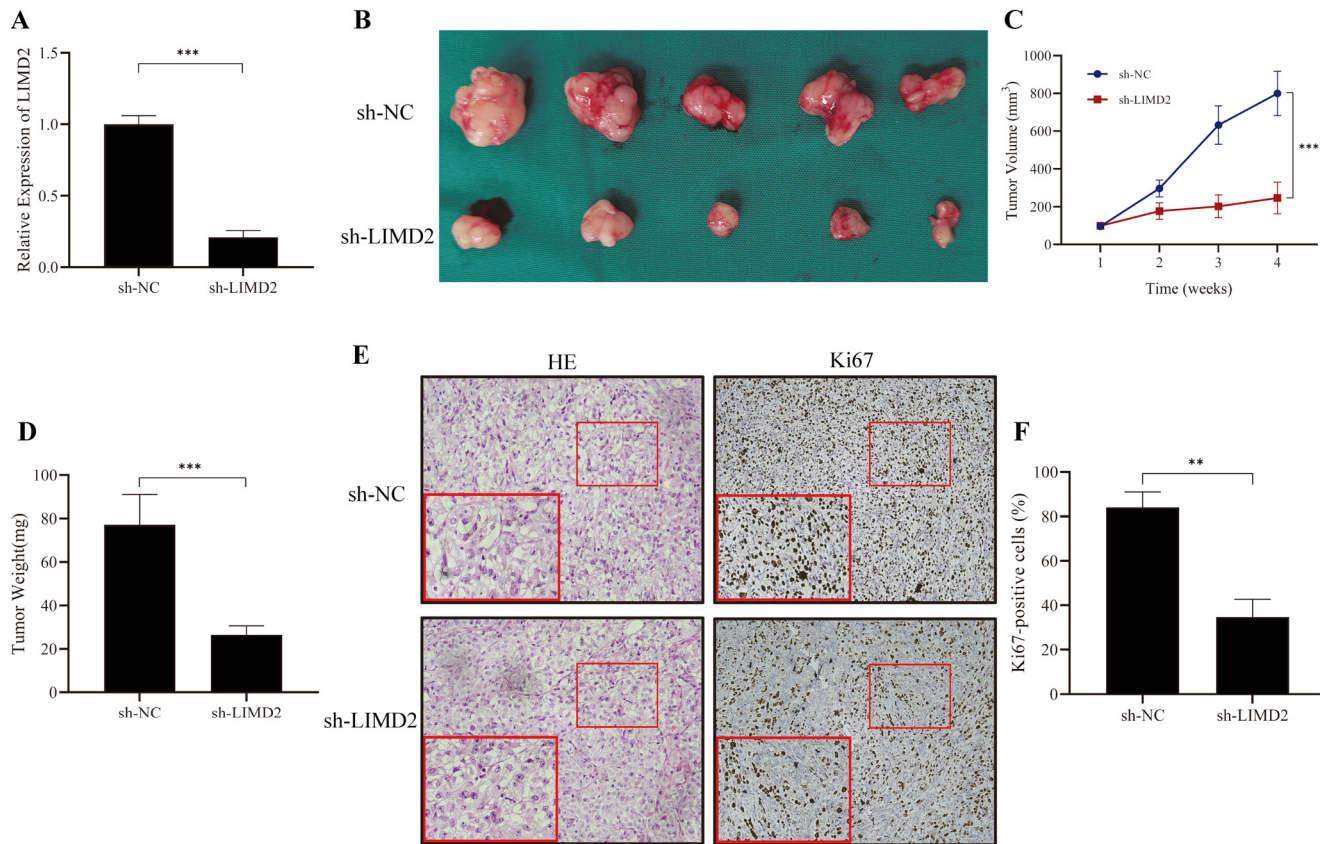
Figure 4. LIMD2 drives tumorigenesis of ccRCC *in vivo*. A) The efficiencies of LIMD2 knockdown in Caki-1 stably transfected with sh-LIMD2. **B)** Gross appearance of xenograft tumors (n=5 per group). **C, D)** Tumor volumes (C) and weights (D) were measured in sh-NC and sh-LIMD2 groups (n=5/group). **E)** Paraffin-embedded sections were stained for Ki-67. **F)** The stained cells were counted and the percentage of Ki67 positive cells was gained. ***p<0.01

SIGNALING". We then attempted to investigate whether LIMD2 promoted EMT in ccRCC. Western blotting analyses were conducted to detect the expression of EMT markers. We discovered that LIMD2 silencing substantially upregulated the expression of E-cadherin and induced a significant reduction in N-cadherin, Slug, and Snail expression simultaneously (Figure 5B), suggesting that LIMD2 knockdown suppressed EMT in ccRCC. These results prove that LIMD2 may drive tumorigenesis and progression via EMT.

LIMD2 triggers EMT via activating the ILK/Akt signaling pathway in ccRCC. The Akt pathway is known to be the upstream regulator of EMT. Moreover, integrin-linked kinase (ILK) was reported to contribute to the phosphorylation of Akt on Ser-473 and possesses the ability to phosphorylate Akt directly [13, 14]. Therefore, we speculated that LIMD2 may promote EMT via activating the ILK/Akt signaling in ccRCC. The western blotting assays indicated that the LIMD2 knockdown markedly decreased the levels of phosphorylated Akt (p-Akt) whereas the protein levels of ILK showed no changes (Figure 5C).

Previous studies showed that ILK contains an N-terminal ankyrin repeat domain (ARD), which could directly bind to a

LIM-domain, therefore activate ILK [15]. Peng et al. reported that LIMD2 could directly bind to ILK and activate ILK in a dose-dependent manner in fibroblasts [8]. In ccRCC, we further discovered that LIMD2 knockdown did not affect the protein level of ILK while the addition of LIMD2 increased the phosphorylation of Akt. Additionally, the effect on p-Akt by exogenous LIMD2 was abolished when OSU-T315, a molecule inhibitor of ILK, was added (Figure 5D). All these findings indicate that LIMD2 may promote proliferation, migration, invasion, and EMT of ccRCC cells via activating the ILK/Akt signaling.

Discussion

LIMD2, a member of the LIM domain-proteins family, is found to be overexpressed and participate in tumorigenesis and progression of a variety of malignant human tumors [7]. LIMD2 is shown as a metastasis-associated protein. Pinheiro et al. reported that LIMD2 was overexpressed in papillary thyroid carcinomas (PTC) and metastasis samples [9]. Zhang et al. found that overexpression of LIMD2 promotes tumor progression, induced the malignant phenotypes of non-small
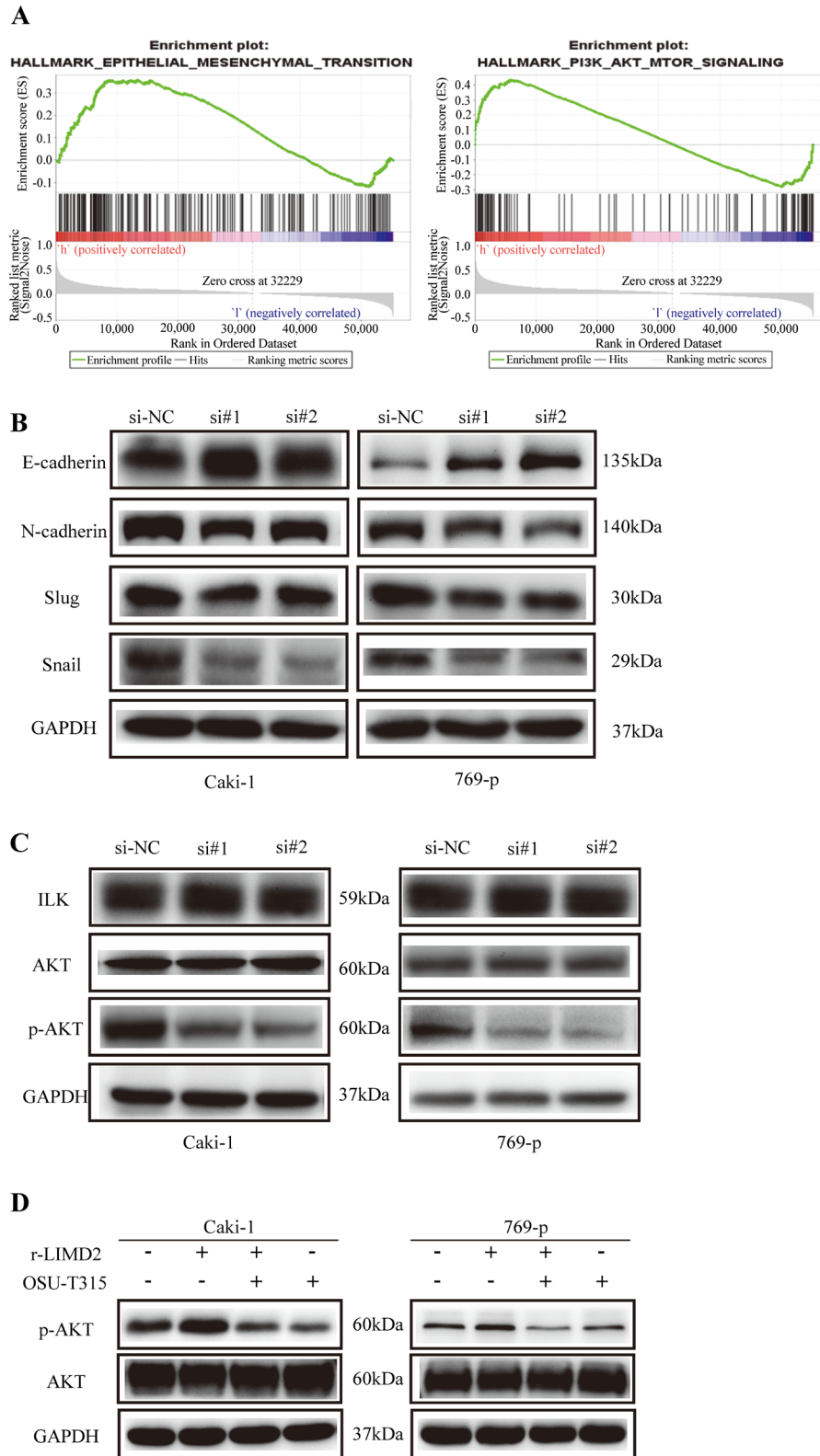
A

B

C

D

Figure 5. LIMD2 triggers EMT via activating the ILK/Akt signaling pathway in ccRCC. A) Significant pathways that positively correlated with high LIMD2 expression. **B)** Western blotting analysis for EMT-related markers in Caki-1 and 769-p cells with LIMD2 silencing. **C)** The effects of OSU-T315, a molecule inhibitor of ILK, on the phosphorylation of Akt by LIMD2.

cell lung cancers (NSCLC) cells, and was linked to a poor prognosis [11]. However, the biological function of LIMD2 in ccRCC remains elusive.

In this study, we discovered the augmenting expression levels of LIMD2 in ccRCC. Moreover, increased LIMD2 expression is linked to a poor clinical outcome of ccRCC, suggesting that LIMD2 may serve as an oncogene of ccRCC. To further investigate the oncogenic role of LIMD2 in ccRCC, we conducted a series of experiments. Consistent with previous studies on other malignancies, we discovered that LIMD2 silencing significantly suppressed the proliferation, migration, and invasion of ccRCC cells *in vitro* and *in vivo*. These results indicated that LIMD2 drives tumorigenesis and progression in ccRCC.

Considering that LIMD2 functioned as a tumor promotive role in ccRCC, we utilized gene set enrichment analysis to explore possible related pathways. We found that the EMT pathway and the Akt pathway were positively correlated with high LIMD2 expression. The EMT process, characterized as the loss of epithelial markers and the increase of mesenchymal markers, is critically related to tumor progression and metastasis [16–18]. In this study, we discovered that LIMD2 knockdown substantially increased the expression of E-cadherin and decreased the expression of N-cadherin, Slug, and Snail suggesting that the LIMD2 knockdown suppressed EMT in ccRCC. These results suggest that LIMD2 may be an EMT inducer.

This study confirmed the oncogene function of LIMD2 in ccRCC. Moreover, integrin-linked kinase (ILK) contains an N-terminal ankyrin repeat domain that can directly bind to a LIM-domain, suggesting that LIM-domain proteins are able to bind to ILK [15]. Previous research reported that LIMD2 could directly bind to ILK in fibroblast cells and activate ILK in a dose-dependent manner [8]. In this study, we further discovered that the LIMD2 knockdown decreased the levels of p-Akt but failed to affect the protein level of ILK in ccRCC. Additionally, exogenous LIMD2 increased the phosphorylation of Akt, but the effect on p-Akt by LIMD2 was abolished when a molecule inhibitor of ILK, OSU-T315, was added. All these findings indicate that LIMD2 may promote proliferation, migration, invasion, and EMT of ccRCC cells via activating the ILK/Akt signaling.

In conclusion, our findings confirmed the oncogenic role of LIMD2 in ccRCC. Additionally, LIMD2 induces the EMT process and activates the ILK/Akt signaling pathway in ccRCC. All these findings indicate that LIMD2 may promote proliferation, migration, invasion, and EMT of ccRCC cells via the ILK/Akt signaling and may function as a novel potential therapeutic target for ccRCC.

References

[1] SIEGEL RL, MILLER KD, JEMAL A. Cancer statistics, 2020. CA Cancer J Clin 2020; 70: 7–30. https://doi.org/10.3322/caac.21590

[2] LINEHAN WM, RICKETTS CJ. The Cancer Genome Atlas of renal cell carcinoma: findings and clinical implications. Nat Rev Urol 2019; 16: 539–552. https://doi.org/10.1038/s41585-019-0211-5

[3] CAPITANIO U, MONTORSI F. Renal cancer. Lancet 2016; 387: 894–906. https://doi.org/10.1016/S0140-6736(15)00046-X.

[4] MILLER KD, NOGUEIRA L, MARIOTTO AB, ROWLAND JH, YABROFF KR et al. Cancer treatment and survivorship statistics, 2019. CA Cancer J Clin 2019; 69: 363–385. https://doi.org/10.3322/caac.21565

[5] WALLIS CJD, KLAASSEN Z, BHINDI B, YE XY, CHANDRASEKAR T et al. First-line Systemic Therapy for Metastatic Renal Cell Carcinoma: A Systematic Review and Network Meta-analysis. Eur Urol 2018; 74: 309–321. https://doi.org/10.1016/j.eururo.2018.03.036

[6] MATTHEWS JM, LESTER K, JOSEPH S, CURTIS DJ. LIM-domain-only proteins in cancer. Nat Rev Cancer 2013; 13: 111–122. https://doi.org/10.1038/nrc3418

[7] CERUTTI JM, OLER G, MICHALUART P JR, DELCELO R, BEATY RM et al. Molecular profiling of matched samples identifies biomarkers of papillary thyroid carcinoma lymph node metastasis. Cancer Res 2007; 67: 7885–7892. https://doi.org/10.1158/0008-5472.CAN-06-4771

[8] PENG H, TALEBZADEH-FARROOJI M, OSBORNE MJ, PROKOP JW, MCDONALD PC et al. LIMD2 is a small LIM-only protein overexpressed in metastatic lesions that regulates cell motility and tumor progression by directly binding to and activating the integrin-linked kinase. Cancer Res 2014; 74: 1390–1403. https://doi.org/10.1158/0008-5472.CAN-13-1275

[9] PINHEIRO DOS SANTOS MJC, BASTOS AU, DA COSTA VR, DELCELO R, LINDSEY SC et al. LIMD2 Is Overexpressed in BRAF V600E-Positive Papillary Thyroid Carcinomas and Matched Lymph Node Metastases. Endocr Pathol 2018; 29: 222–230. https://doi.org/10.1007/s12022-018-9526-7

[10] WANG F, LI Z, XU L, LI Y, LI Y et al. LIMD2 targeted by miR34a promotes the proliferation and invasion of nonsmall cell lung cancer cells. Mol Med Rep 2018; 18: 4760–4766. https://doi.org/10.3892/mmr.2018.9464

[11] ZHANG F, QIN S, XIAO X, TAN Y, HAO P et al. Overexpression of LIMD2 promotes the progression of non-small cell lung cancer. Oncol Lett 2019; 18: 2073–2081. https://doi.org/10.3892/ol.2019.10473

[12] ARALDI RP, DE MELO TC, LEVY D, DE SOUZA DM, MAURICIO B et al. LIMD2 Regulates Key Steps of Metastasis Cascade in Papillary Thyroid Cancer Cells via MAPK Crosstalk. Cells 2020; 9: 2522. https://doi.org/10.3390/cells9112522

[13] PERSAD S, ATTWELL S, GRAY V, MAWJI N, DENG JT et al. Regulation of protein kinase B/Akt-serine 473 phosphorylation by integrin-linked kinase: critical roles for kinase activity and amino acids arginine 211 and serine 343. J Biol Chem 2001; 276: 27462–27469. https://doi.org/10.1074/jbc.M102940200

[14] TROUSSARD AA, MAWJI NM, ONG C, MUI A, ST-AR-NAUD R et al. Conditional knock-out of integrin-linked kinase demonstrates an essential role in protein kinase B/Akt activation. J Biol Chem 2003; 278: 22374–22378. https://doi.org/10.1074/jbc.M303083200

[15] HANNIGAN GE, LEUNG-HAGESTEIJN C, FITZ-GIBBON L, COPPOLINO MG, RADEVA G et al. Regulation of cell adhesion and anchorage-dependent growth by a new beta 1-integrin-linked protein kinase. Nature 1996; 379: 91–96. https://doi.org/10.1038/379091a0

[16] AIELLO NM, BRABLETZ T, KANG Y, NIETO MA, WEINBERG RA et al. Upholding a role for EMT in pancreatic cancer metastasis. Nature 2017; 547: E7–E8. https://doi.org/10.1038/nature22963

[17] YE X, BRABLETZ T, KANG Y, LONGMORE GD, NIETO MA et al. Upholding a role for EMT in breast cancer metastasis. Nature 2017; 547: E1–E3. https://doi.org/10.1038/nature22816

[18] PASTUSHENKO I, BRISEBARRE A, SIFRIM A, FIORAMONTI M, REVENCO T et al. Identification of the tumour transition states occurring during EMT. Nature 2018; 556: 463–468. https://doi.org/10.1038/s41586-018-0040-3